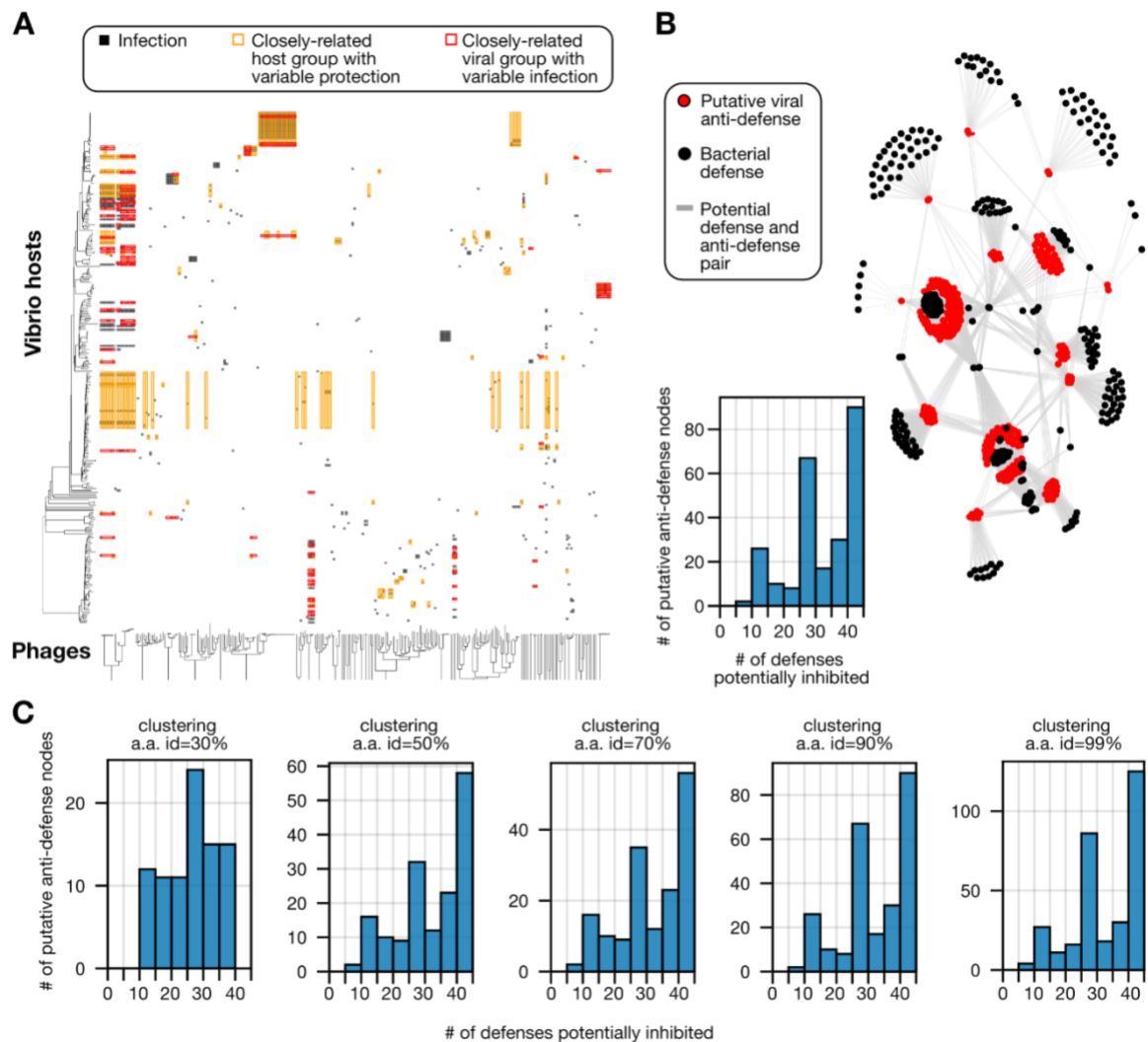


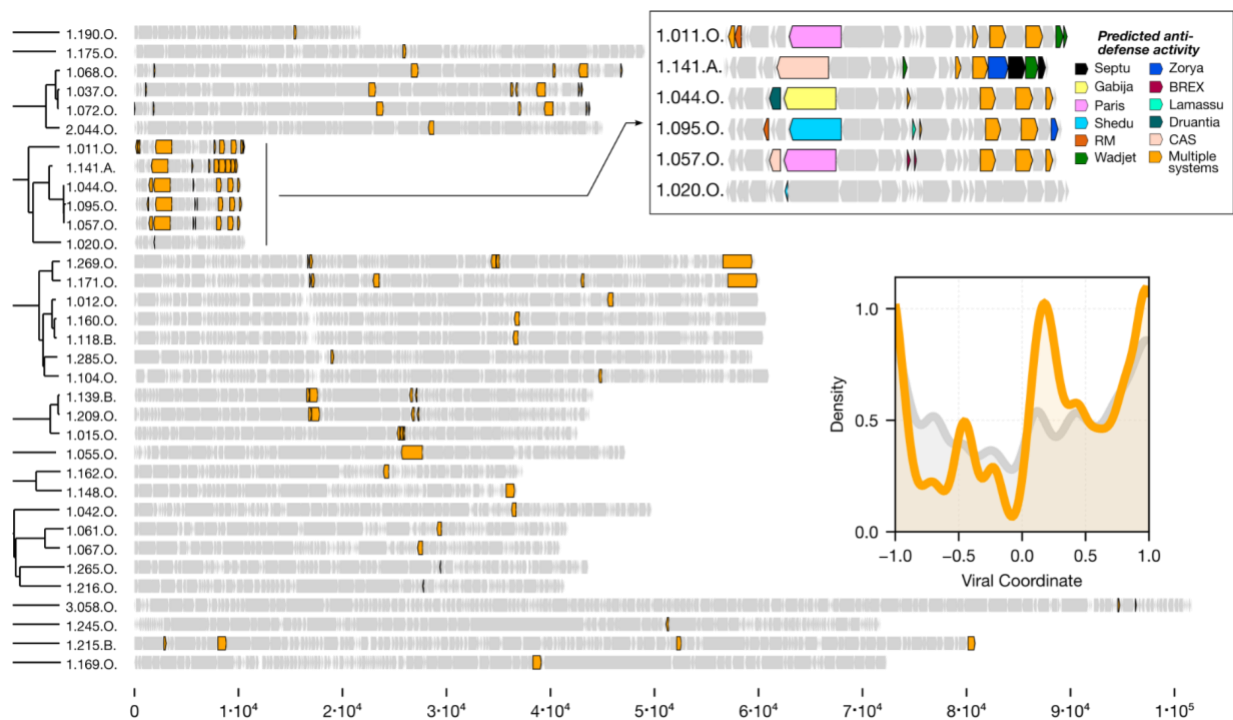
Extended Data Figure 1. Associating bacterial defenses to putative viral anti-defense genes
is limited by the high number of defenses co-occurring in bacterial genomes.



Extended Data Figure 1. Associating bacterial defenses to putative viral anti-defense genes
is limited by the high number of defenses co-occurring in bacterial genomes. **a**, The Nahant cross-infection matrix with relevant closely related viral (phage, x-axis) and bacterial groups (y-axis) highlighted. The trees represent FastME dendrograms built from ANI distances. Entries in the matrix are marked with a black box if a particular phage can infect and lyse a particular bacterial host. Groups of closely related phages (average ANI ≥ 0.95) that differentially infect a

10 particular bacterial host are marked on the matrix with a red rectangle surrounding the relevant
11 infection data of the phage group and the host. Closely related bacteria (Average ANI ≥ 0.95)
12 that are differentially protected from a single phage are marked in the same way using golden
13 rectangles. Putative anti-defenses are identified within each phage group, potential inhibitory
14 interactions are identified across all genomes (methods). **b**, Network showing connections
15 between bacterial defenses and the putative viral anti-defenses that inhibit them based on a
16 comparative genomic analysis of the Nahant cross-infection matrix. Putative anti-defense genes
17 (red nodes) in viral genomes were identified as gene families (clustered at 90% identity) found
18 only in viruses infecting a single bacterial host, compared to their close relatives that do not
19 infect that host (methods). Bacterial defenses (black nodes) in each host were identified using
20 DefenseFinder, and links are drawn between putative anti-defenses and the defenses encoded in
21 the infected host. The histogram shows the degree distribution of each anti-defense, i.e., how
22 many defenses it putatively inhibits. Identifying specific inhibition of defenses by anti-defenses
23 would require extensive trial and error genetics approaches. **c**, putative anti-defense node degree
24 histograms for different protein clustering amino-acid (a.a) similarity thresholds (indicated at the
25 top of each histogram). The distributions are very skewed towards high values for all thresholds,
26 and there are no clear-cut cases of defense and anti-defense pairs in any threshold.

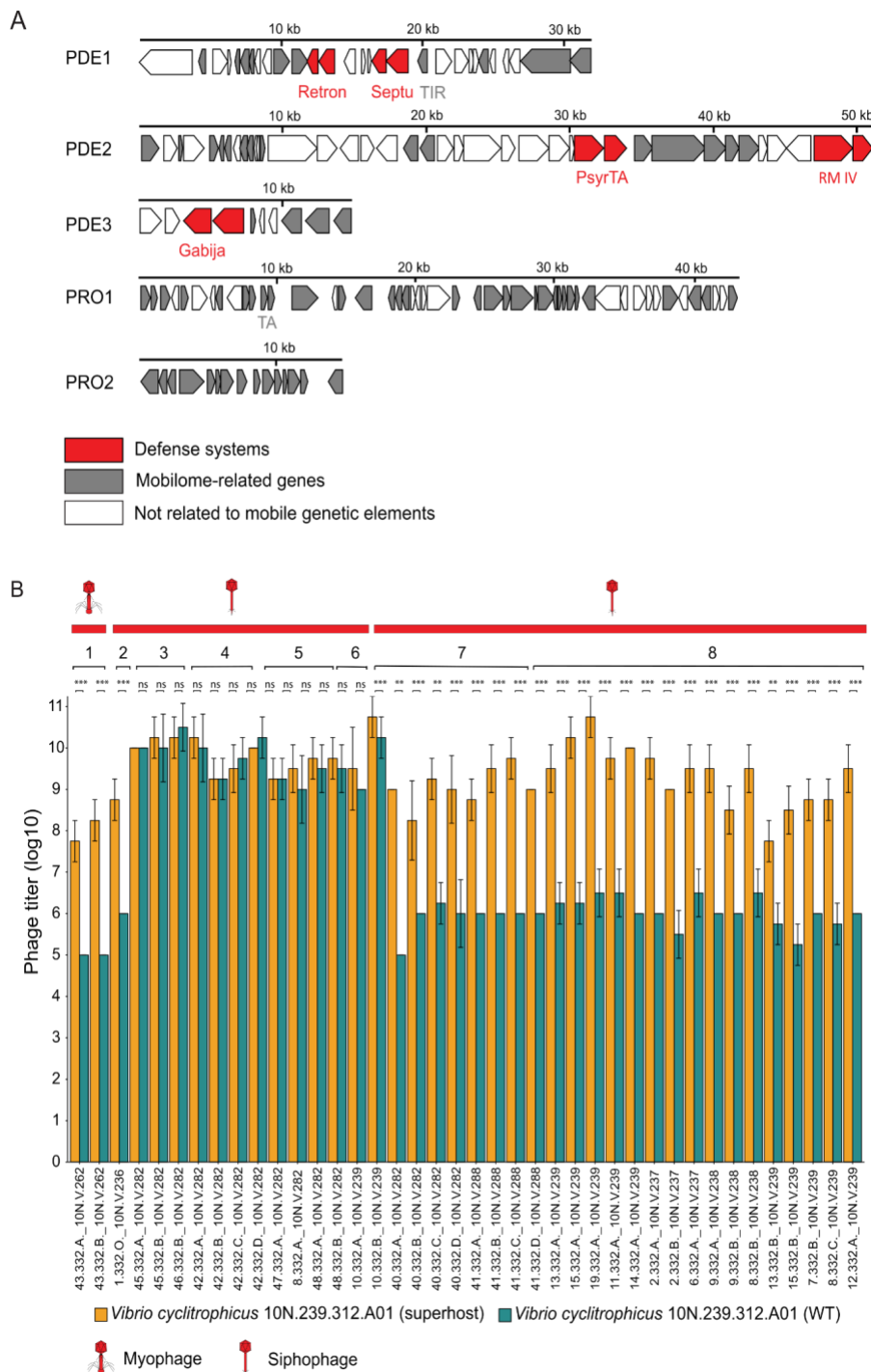
Extended Data Figure 2. Mapping of putative anti defenses identified by VirMAD onto viral genomes of the Nahant cross-infection matrix.



Extended Data Figure 2. Mapping of putative anti defenses identified by VirMAD onto

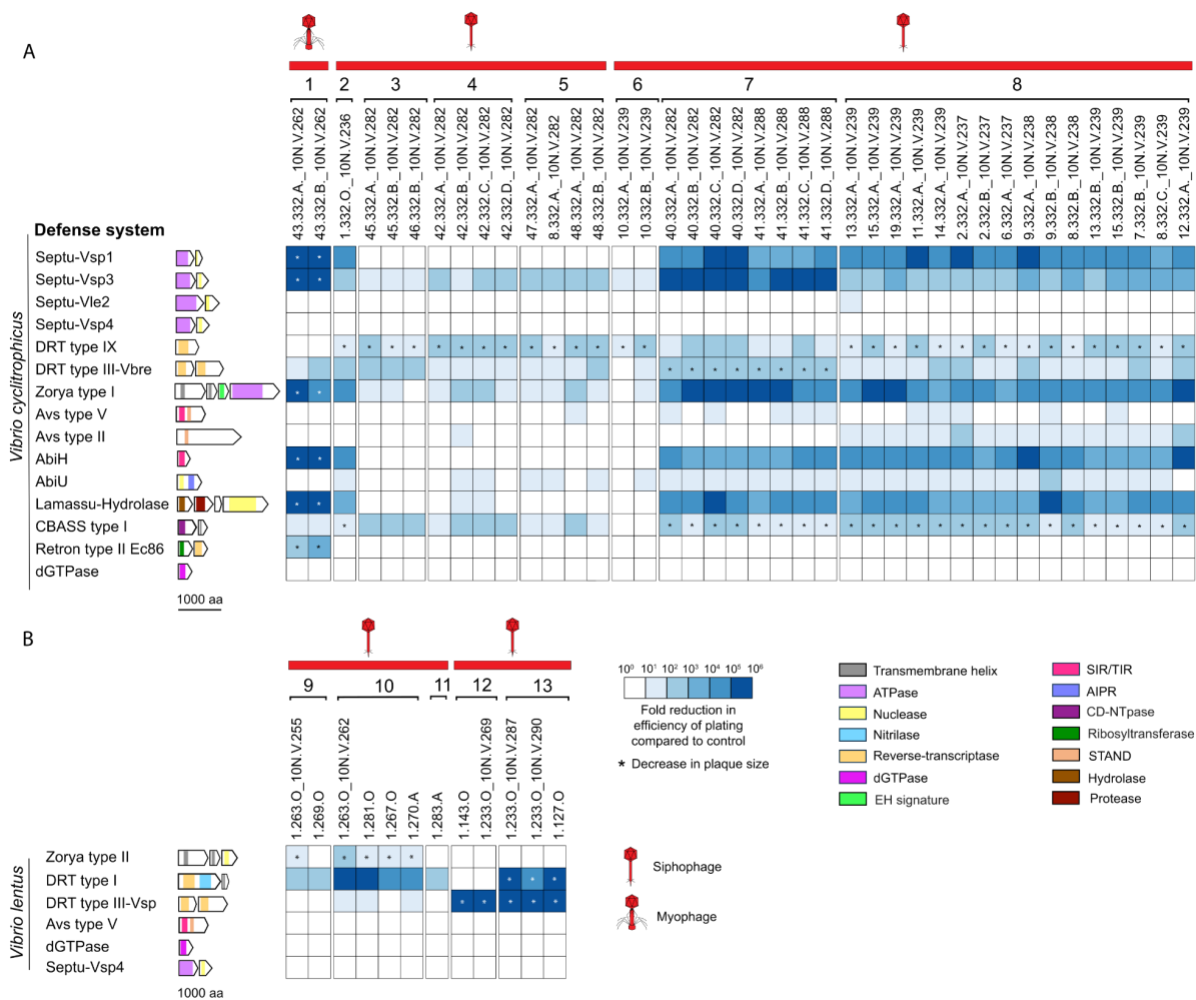
viral genomes of the Nahant cross-infection matrix. The tree on the left was built using fastME⁶⁸ based on ANI values between full viral genomes. Clades that are disconnected have no detectable homology to viruses from other clades. Only viruses that contained homologues (>90% a.a similarity) of putative anti-defenses are shown. Each row represents a viral genome, starting at the viral terminase small subunit with arrows representing genes to scale as marked in the bottom. The highlighted viruses have short genomes, which contain many putative anti-defenses with different specificities. The density plot on the right shows the normalized position of putative anti-defenses (orange curve) in the viral genomes compared to all genes (gray curve).

Extended Data Figure 3. Deletion of phage defense systems in the superhost results in increased phage sensitivity



Extended Data Figure 3. Deletion of phage defense systems in the superhost results in increased phage sensitivity **a**, Creation of the superhost strain by deletion of mobile genetic elements from *Vibrio cyclitrophicus* 10N.239.312.A01, chosen because they either contained predicted defenses or represented prophages. Arrow gene diagrams drawn to scale (annotations are in Supplementary Table 10). **b**, Comparison of titers of 40 viruses on wild type (teal) and superhost (orange) showing increased susceptibility of the superhost. Numbers under red bars represent clusters of viruses based on genome similarity (Supplementary Table 16). Data represent average of three independent replicates with standard deviations (s.d.) shown as vertical error bars.

Extended Data Figure 4. Fold-protection conferred by all experimentally verified defense systems

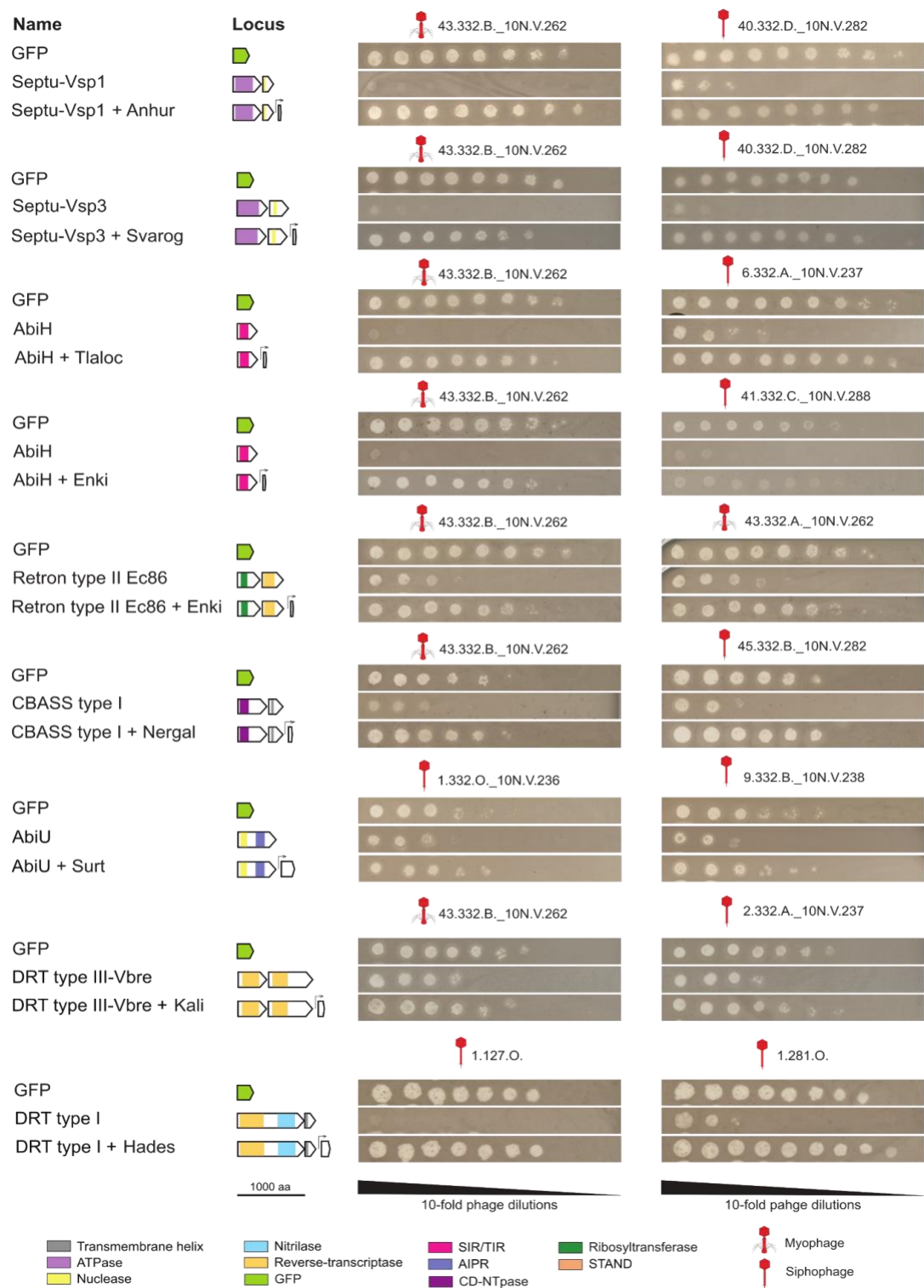


Extended Data Figure 4. Fold-protection conferred by all experimentally verified defense systems

Defenses expressed in **a**, the *Vibrio cyclitrophicus* superhost and **b**, *Vibrio lentus* $\Delta 3$ (methods). The strength of protection is shown as a heatmap where values correspond to the fold change in efficiency of plating (measured in serial dilution plaque assays) compared to an unprotected host (GFP expressing plasmid) for each virus. Numbers above virus identifiers represent clusters of viruses based on genome similarity (Supplementary Table 16). Data

62 represent the average of three replicates (examples of raw data shown in Supplementary Fig. 1).
63 Asterisks (*) indicate significant reduction in plaque size. Arrow gene diagrams with predicted
64 protein domains in color are drawn to scale.

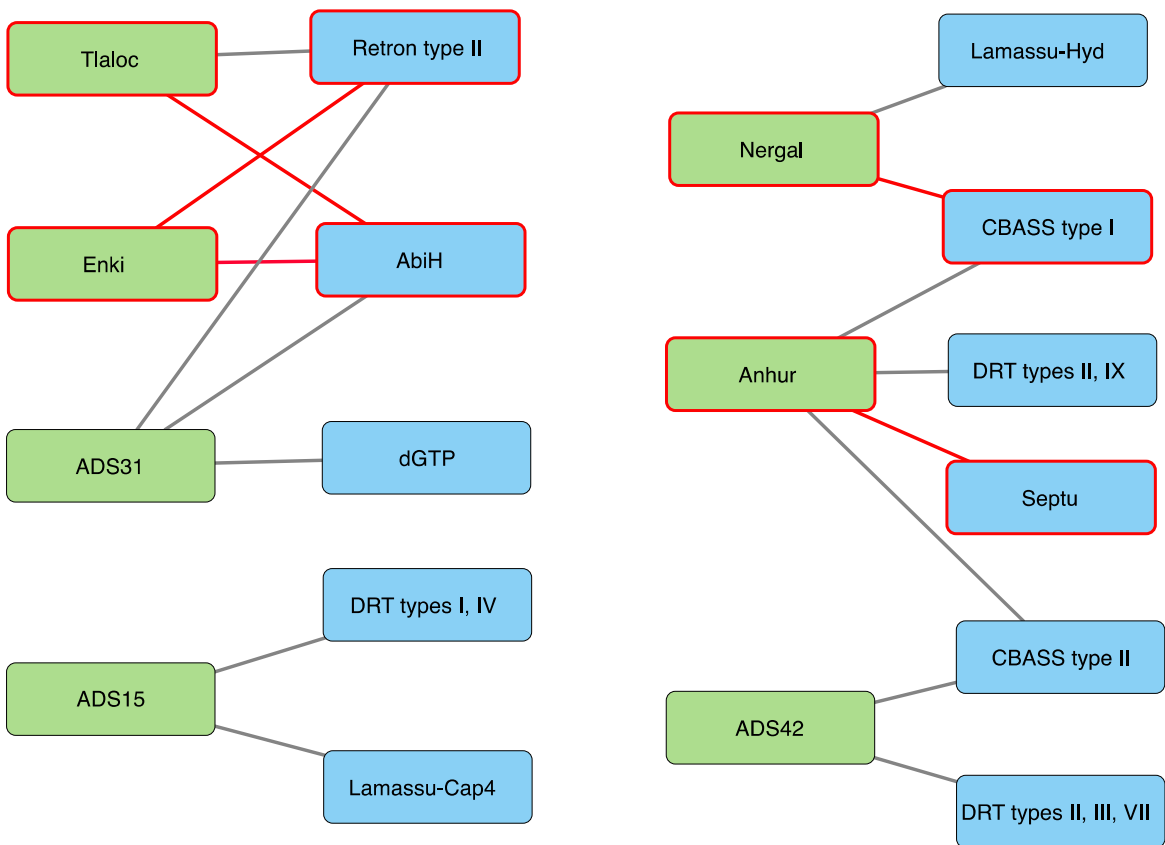
65 **Extended Data Figure 5. Drop spots of 10-fold serially diluted viruses on hosts expressing**
 66 **GFP (control), defense systems or paired defense systems and anti-defense proteins.**



68 **Extended Data Figure 5. Drop spots of 10-fold serially diluted viruses on hosts expressing**
69 **GFP (control), defense systems or paired defense systems and anti-defense proteins.**

70 This figure accompanies Fig. 2 and Extended Fig. 4. For each paired defense and anti-defense,
71 the two viruses are shown for which the defense system provided the strongest protection. Plaque
72 assays are representative of three independent replicates. Arrow gene diagrams with predicted
73 protein domains in color are drawn to scale.

Extended Data Figure 6. Anti-defense proteins with multiple non-homologous targets, and defense systems with multiple non-homologous inhibitors.



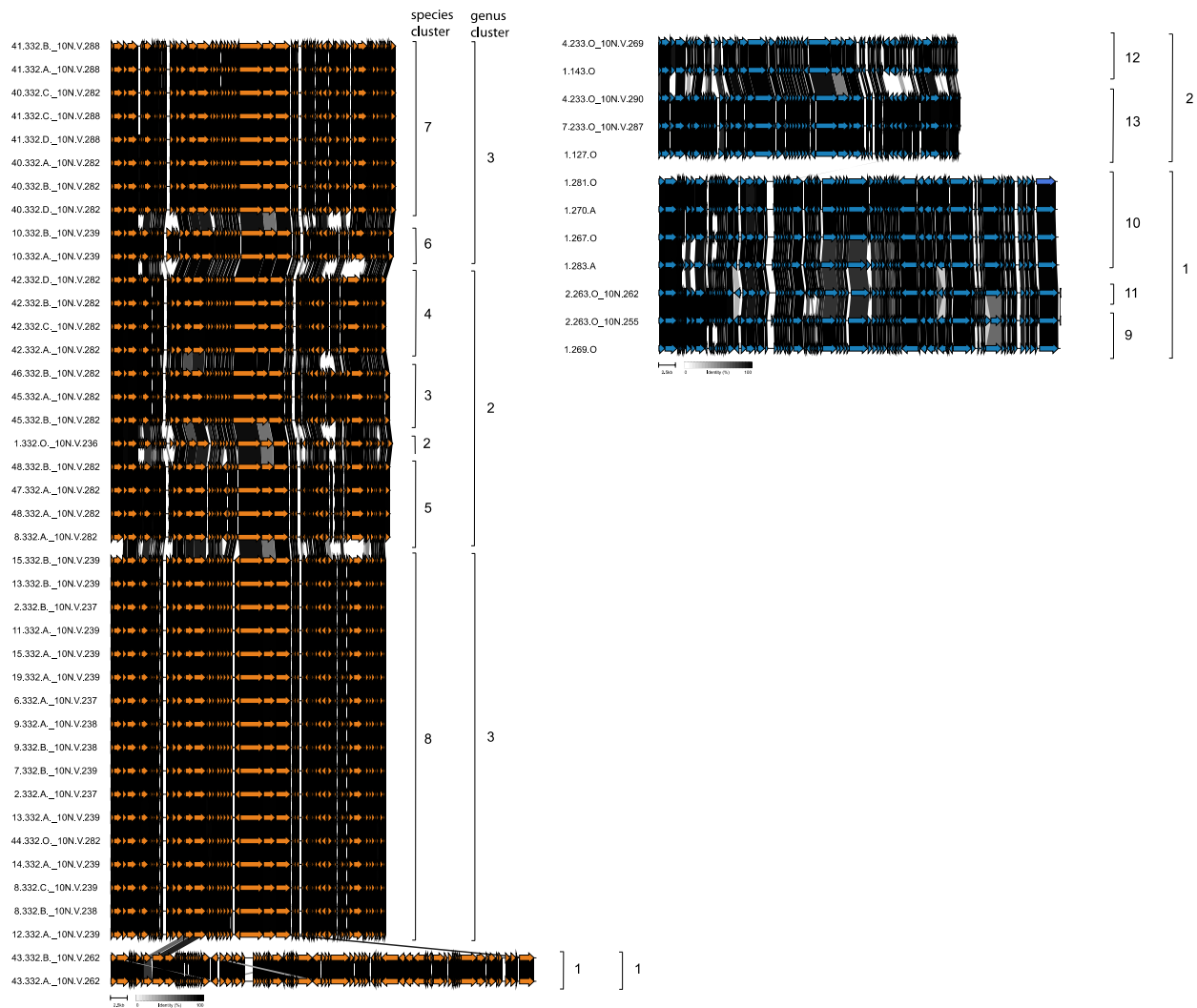
Extended Data Fig. 6. Anti-defense proteins with multiple non-homologous targets, and defense systems with multiple non-homologous inhibitors. The network shows highly scored (>80) VirMAD predictions of defense-anti-defense pairs for ten defense systems chosen for experimental verifications. Only anti-defense proteins with two or more predicted types of defense systems are shown in the network. Putative anti-defense proteins (green boxes) are clustered at 95% sequence similarity, while defense systems (blue boxes) were classified into subtypes using DefenseFinder (see Supplementary Tables 1 and 4). Red lines correspond to defense-anti-defense pairs which were experientially verified.

86 **Supplementary Figure 1. Raw data for fold-protection calculation.**

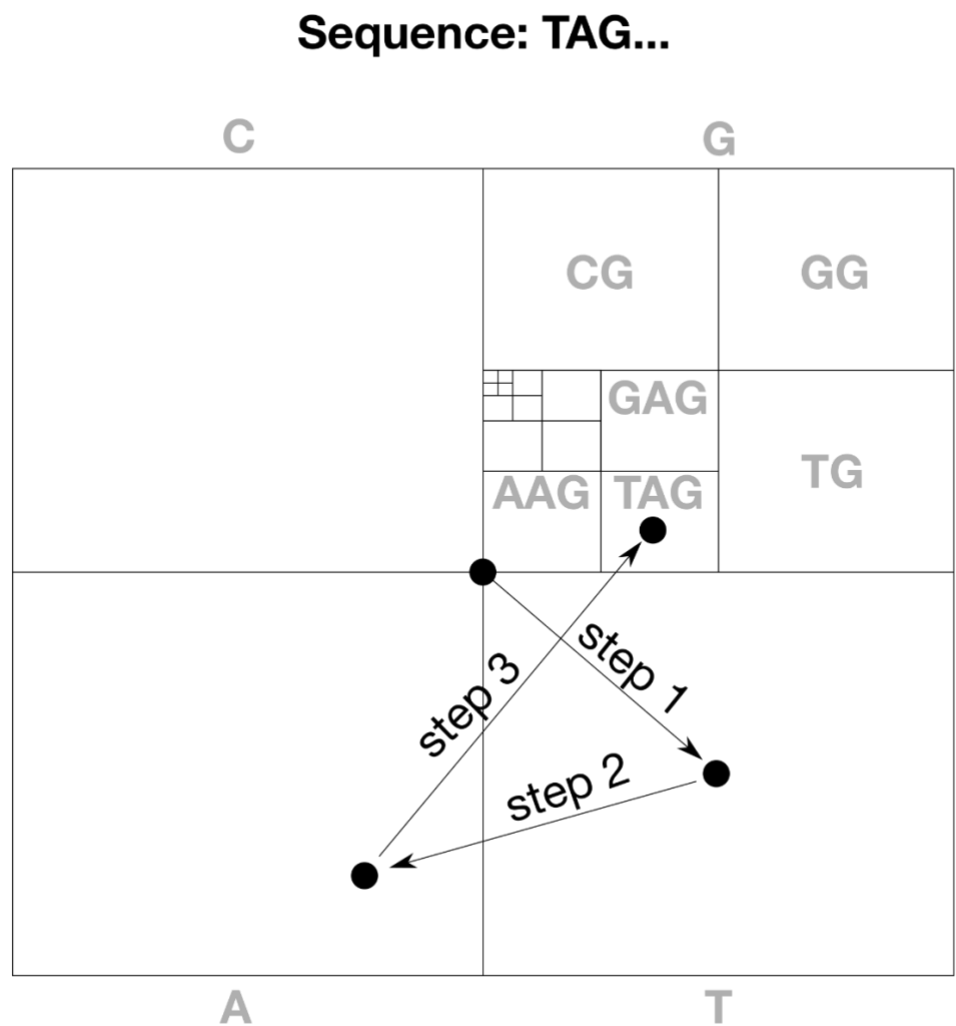


88 **Supplementary Fig. 1. Raw data for fold-protection calculation.** This figure accompanies
89 Fig. 2 and Extended Fig. 4. Defense systems expressed in **a**, *Vibrio cyclitrophicus* superhost and
90 **b**, *V. lentus* $\Delta 3$ (see Methods). Fold-protection data for all verified pairs of defense systems and
91 anti-defense proteins were obtained for 40 viruses for the superhost strain and 12 viruses for the
92 $\Delta 3$ strain. Plaque-forming units were measured for each virus on hosts containing either a GFP-
93 expressing control plasmid (grey), a defense-expressing plasmid (red), or a plasmid expressing
94 both the defense system and anti-defense protein (green). Data represent an average of three
95 independent replicates with standard deviations (s.d.) shown as a vertical bars. All defense
96 systems were expressed from their native promoters, while anti-defense genes were under the
97 control of an inducible *PlacI* promoter. Virus titers were measured after 24 hours of incubation at
98 25°C.

Supplementary Figure 2. Genomic diversity of *Vibrio cyclitrophicus* and *V. lentus* viruses used in plaque assays.



Supplementary Fig. 2. Genomic diversity of *Vibrio cyclitrophicus* and *V. lentus* viruses used in plaque assays. Genomic comparison of the 40 viruses infecting *Vibrio cyclitrophicus* superhost (orange) and the 12 viruses infecting *Vibrio lentus* $\Delta 3$ (blue) used in experiments underlying the data in Fig. 2 and Extended Fig. 4. Grey shading indicates the percent identity between homologous proteins. Species and genus cluster predictions (Viridic) are shown on the right.



109

110 **Supplementary Fig. 3. Chaos Game Representation of nucleotide sequences.** To visually

111 represent nucleotide sequences, each corner of a square is assigned to a nucleotide. Starting out

112 in the middle of the square, the sequence is processed one base at a time, each time going from

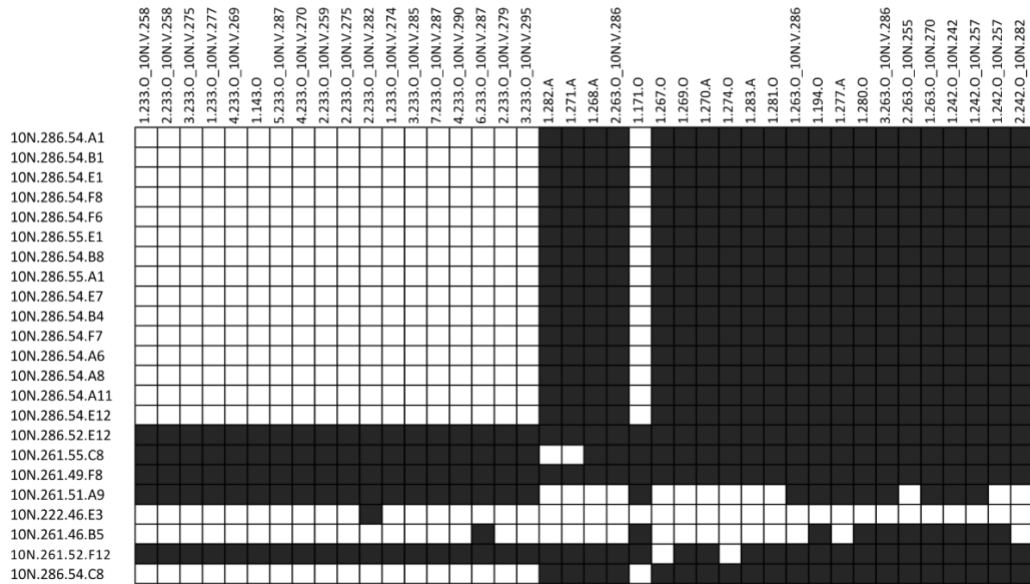
113 the current location halfway to the corner representing the nucleotide being processed. This

114 creates fractal regions corresponding to increasingly long k-mers, as represented in the figure

115 with smaller and smaller squares that divide the total area of the figure. An illustration is

116 provided for the first 3 steps in a sequence that starts with the nucleotides TAG.

Supplementary Figure 4. Virus-host cross-infection matrix supplementing the Nahant matrix.



Supplementary Fig. 4. Virus-host cross-infection matrix supplementing the Nahant matrix.

Forty viruses were isolated on 5 *Vibrio lentus* strains (methods) and tested against an extended set of 25 *V. lentus* isolates. Positive interactions (lysis) are shown as dark-grey square and negative interactions as white squares. Bacterial strains are ordered based on phylogeny of concatenated single copy ribosomal protein genes; viruses are ordered based on manual sorting of VIRIDIC genus-level trees. This additional matrix was used in the VirMAD predictions.

Supplementary Tables

Supplementary Table 1. Nine known anti-defense proteins used as positive controls for model predictions.

VirMAD score	Defense system	Defense protein	Defense protein ID	Anti-defense protein	Virus	Virus protein ID
93,6	DSR2	DSR2	API95927.1	DSAD1	SPBc2	AAC13153.1
99,1	Gabija	GajA	EJQ91274.1	Gad1	phi3T	APD21271.1
		GajB	EJQ91275.1			
80,0	Hachiman	HamA	KLA13163.1	Had1	SBSphiJ4	UPI12729.1
		HamB	KLA13162.1			
73,4	Thoeris	ThsA	EJR09240.1	Tad2	SPO1	YP_002300464.1
		ThsB	EJR09241.1			
70,0	Thoeris	ThsA	EJR09240.1	Tad1	SBSphiJ7	UPI13470.1
		ThsB	EJR09241.1			
68,4	Gabija	GajA	EJQ91274.1	Gad2	SPbetaL7	WIT28108.1
		GajB	EJQ91275.1			
NA	CBASS	Cyclase	CAP15_YERAE	Acb1	T4	AAD42501.1
		Cap15	CDNE_YERAE			
NA	Pycsar	PycA	WP_001682322.1	Apyc1	SBSphiJ	APYC1_BPSBS
		PycB	WP_053265929.1			
NA	CBASS	Cap2	P0DX87.1	Acb2	PaMx33	ANA48877.1
		CdnA	P0DX86.1			
		CapV	P0DX85.1			

*NA - confidence of predictions too low

132 **Supplementary Table 2. Relative abundance of defense systems in 758 *Vibrio* genomes from the**
133 **Nahant collection.**

Defense system type	% relative abundance	VirMAD prediction	Experimental verification of defense phenotype
Restriction-modification	35,9	YES	
dGTPase	13,6	YES	YES
Septu	7,1	YES	YES
CRISPR	4,9	YES	
Gabija	4,3	YES	
CBASS	3,8	YES	YES
Retron	3,7	YES	YES
Wadjet	2,6	YES	
DRT	2,4	YES	YES
Dnd	2,0	YES	
AbiH	1,4	YES	YES
Rst_PARIS	1,3	YES	
Zorya	1,3	YES	YES
Hachiman	1,1		
SspBCDE	1,1		
Kiwa	1,0		
Shedu	0,9	YES	
Lit	0,8		
Druantia	0,8	YES	
Viperin	0,8		
DarTG	0,7		
dCTPdeaminase	0,7		
Avs	0,7	YES	YES

Gao_Ppl	0,6		
BREX	0,6	YES	
AbiU	0,5	YES	YES
Thoeris	0,5		
Dsr	0,5		
Gao_Hhe	0,4		
Rst_3HP	0,4		
Lamassu	0,4	YES	YES
Gao_Qat	0,4		
PrrC	0,3		
AbiEii	0,3		
Gao_Her	0,3		
Gao_Ape	0,3		
Gao_Tmn	0,3		
RADAR	0,3		
Rst_DprA-PPRT	0,2		
Rst_HelicaseDUF2290	0,2		
Rst_DUF4238	0,2		
BstA	0,1		
DISARM	0,1		
Gao_Iet	0,1		
Gao_RL	0,1		
Nhi	0,1		
Rst_TIR-NLR	0,1		
Gao_Mza	0,1		
Gao_Upx	0,1		
Rst_Hydrolase-3Tm	0,1		

135 **Supplementary Table 3. Number of putative anti-defense proteins predicted by the VirMAD model**
136 **for 19 defense system types**

Defense system name	Number of putative anti-defense proteins 137	
	score >50	score >80
AbiH	8	3
AbiU	2	0
Avs	10	1
Brex	11	1
CBASS	34	4
CRISPR	54	45
dGTP	12	1
DND	13	1
DRT	37	10
Druantia	3	2
Gabija	20	13
Lamassu	5	2
Paris	11	6
Retron	26	4
RM	71	6
Septu	53	7
Shedu	7	3
Wadjet	22	4
Zorya	17	5

139 **Supplementary Table 4. Cloned defense systems and putative anti-defense proteins.**

Defense type	Abundance rank ¹	Subtype	Vibrio strain ²	Defense ³		Anti-defense ³			
				Cloned	Phenotype	Score	Cloned	Phenotype	Name ⁴
Septu	3	Vsp1*	<i>Vibrio</i> sp. F13 10N.222.55.C6	Y	Y	86.8	Y	Y	Anhur
		Vle2*	<i>V. lentus</i> 10N.286.52.E8	Y	N	88.8			
		Vsp3*	<i>V. splendidus</i> 10N.261.46.F	Y	Y	81.3	Y	Y	Svarog
		Vsp4*	<i>Vibrio</i> sp. F13 10N.222.54.A6	Y	N	100.0			
DRT	9	Type I	<i>V. lentus</i> 10N.261.45.F4	Y	Y	85.7	Y	Y	Hades
		Type III-Vsp*	<i>V. sp</i> 10N.286.54.E3	Y	Y	96.6	N		
		Type IX	<i>Vibrio</i> sp. 10N.222.51.F6						
		Type III-Vbre*	<i>V. breoganii</i> 10N.261.51.E6	Y	Y	57.7	Y	Y	Kali
AbiH	11		<i>Vibrio</i> sp. 10N.286.45.F3	Y	Y	94.8	Y	Y	Enki
			<i>Vibrio</i> sp. 10N.286.45.F3	Y	Y	93.0	Y	Y	Tlaloc
Avast	23	Type V	<i>V. breoganii</i> 10N.261.54.C7	Y	Y	100.0	N		
		Type II	<i>Vibrio</i> sp. 62478	Y	Y	52.8	Y	N	
CBASS	6	Type I	<i>V. lentus</i> 10N.286.45.C1	Y	Y	85.2	Y	Y	Nergal
Retron	7	Type II	<i>Vibrio</i> sp. F13 Ec86 10N.222.55.A11	Y	Y	91.9	Y	Y	Enki
			<i>Vibrio</i> sp. F13 10N.222.55.A11	Y	Y	99.6	N		
Zorya	13	Type I	<i>Vibrio</i> sp. F13 10N.222.55.A11	Y	Y				

AbiU	26		<i>V. lentus</i>	Y	Y	56.8	Y	Y	Surt
			10N.261.52.F1						
Lamassu	32	Hydrolase	<i>Vibrio</i> sp.	Y	Y	100.0	N		
		Protease	10N.222.49.C10						
dGTPase	2		<i>V. tasmaniensis</i>	Y	N	62.1			
			10N.261.46.A9						
Negative control									
Zorya	13	Type II	<i>V. sp</i>	Y	Y	-	Y		
			10N.286.46.A10						

140

141 ¹ The abundance of each defense system was determined as a percent composition of a defense system
142 relative to the total number of defense systems in 758 *Vibrio* genomes, see Supplementary Table 2 for the
143 list of defense systems and their percent of abundance.

144 ² Accession numbers for all genomes are in Supplementary Data 2.

145 ³ Y = successful cloning or verified defense phenotype; N = failed cloning or absence of defense
146 phenotype. No entry = not attempted.

147 ⁴ Unique anti-defense proteins were named according to the scheme in Supplementary Table 6.

148 * In cases where multiple operons were cloned for the same type or subtype of defense system, the
149 subtype name was supplemented with an additional descriptor, e.g., Vsp1 – abbreviation for *Vibrio sp* 1
150 according to the systematic nomenclature for Retrons described elsewhere¹.

151

Supplementary Table 5. Experimentally verified anti-defense proteins active against a wide range of defense systems.

Anti-defense protein	Anti-defense cluster number¹	Active against defence system	Derived from phage, ID	Length, aa	Model score
Anhur	ADS36	Septu	1.196.O.	37	86,8
Svarog	ADS43	Septu	1.066.O.	42	81,3
Enki	ADS29	AbiH, Retron type II	1.080.O.	38	93,0/91,9
Tlaloc	ADS30	AbiH	1.056.O.	41	94,8
Nergal	ADS45	CBASS type I	1.209.O.	55	82,2
Surt	ADS32	AbiU	1.217.O.	195	56,8
Kali	ADS4	DRT typeIII	1.139.B.	89	57,5
Hades	ADS46	DRT type I	1.066.O.	125	85,7

¹ see Supplementary Data 2.

156 **Supplementary Table 6. Examples of possible names for anti-defenses in the proposed naming**
157 **scheme based on gods or mythological figures to whom some form of destruction is ascribed.**

God ¹	Ascribed role in religion or mythology ²
Shiva	In Hindu mythology, Shiva is often depicted as the destroyer of the universe, responsible for bringing about the end of cycles of creation.
Sekhmet	In Egyptian mythology, Sekhmet is a lioness-headed goddess associated with war, destruction, and healing.
Hades	In Greek mythology, Hades is the god of the underworld, associated with death and the afterlife.
Kali	In Hindu mythology, Kali is a fierce goddess associated with destruction, time, and change.
Thor	In Norse mythology, Thor is the god of thunder associated with storms, lightning, and destruction.
Anhur	In Egyptian mythology, Anhur is a warrior god associated with war and destruction.
Enki	In Sumerian mythology, Enki is a god associated with water, wisdom, and also with the power to bring about floods and destruction.
Tlaloc	In Aztec mythology, Tlaloc is the god of rain, storms, and water, sometimes associated with destructive floods.
Ares	In Greek mythology, Ares is the god of war, violence, and bloodshed, often associated with destruction on the battlefield.
Mars	In Roman mythology, Mars is the counterpart of Ares, also representing war and destruction.
Set	In Egyptian mythology, Set is a god associated with chaos, storms, and destruction. He is often depicted as a malevolent force.
Surt	In Norse mythology, Surt is a fire giant who plays a significant role in the destruction of the world during Ragnarok, the end of the world.
Eris	In Greek mythology, Eris is the goddess of strife, discord, and chaos, often causing destruction through her actions.

<i>Nergal</i>	In Mesopotamian mythology, Nergal is the god of war and plague, associated with destruction and death.
<i>Svarog</i>	In Slavic mythology, Svarog is a deity associated with fire, blacksmithing, and sometimes destruction.
Tezcatlipoca	In Aztec mythology, Tezcatlipoca is a god associated with night, sorcery, and destruction, often depicted with a smoking mirror representing destruction and fate.
Kraken	A legendary sea monster known for its strength and ability to defeat sailors.
Perseus	A hero in Greek mythology who defeated the Gorgon Medusa with clever tactics.
Fenrir	A monstrous wolf in Norse mythology known for breaking free of chains and causing chaos.
Cu Chulainn	A hero in Irish mythology known for his exceptional skill in battle.
Tiamat	A primordial goddess in Babylonian mythology associated with chaos and overcoming order.
Karna	A warrior in Hindu mythology known for his skill and resilience in battle.
Echidna	A creature in Greek mythology known as the "Mother of Monsters," overcoming various foes.

158

159 ¹ Names used for systems verified here are italicized.

160 ² The description was obtained from ChatGTP (March 2024)

161

162 **Supplementary table 7. Classification of *V.cyclitrophicus* and *V.lentus* phages used in the plaque**
163 **assays.**

Official virus name	Short virus name	Family	Genus	Species	Day of isolation	Genome length, bp	Accession number
1.332.O._10N.239.312.A0	1.332.O._10N.V.23	Nibaviridae	Fabiennevirus	Fabiennevirus	236	41880	PRJNA32810
1.SH1_10N.V.236	6			fabienneuna			2
10.332.A._10N.239.312.A	10.332.A._10N.V.2	Nibaviridae	Ninavirus	Ninavirus	239	41998	PRJNA32810
01.SH1_10N.V.239	39			ninauna			2
10.332.B._10N.239.312.A	10.332.B._10N.V.2	Nibaviridae	Ninavirus	Ninavirus	239	41998	PRJNA32810
01.SH1_10N.V.239	39			ninauna			2
11.332.A._10N.239.312.A	11.332.A._10N.V.2	Nibaviridae	Ninavirus	Ninavirus	239	40889	PRJNA32810
01.SH1_10N.V.239	39			ninaduae			2
12.332.A._10N.239.312.A	12.332.A._10N.V.2	Nibaviridae	Ninavirus	Ninavirus	239	40889	PRJNA32810
01.SH1_10N.V.239	39			ninaduae			2
13.332.A._10N.239.312.A	13.332.A._10N.V.2	Nibaviridae	Ninavirus	Ninavirus	239	40889	PRJNA32810
01.SH1_10N.V.239	39			ninaduae			2
13.332.B._10N.239.312.A	13.332.B._10N.V.2	Nibaviridae	Ninavirus	Ninavirus	239	40889	PRJNA32810
01.SH1_10N.V.239	39			ninaduae			2
14.332.A._10N.239.312.A	14.332.A._10N.V.2	Nibaviridae	Ninavirus	Ninavirus	239	40889	PRJNA32810
01.SH1_10N.V.239	39			ninaduae			2
15.332.A._10N.239.312.A	15.332.A._10N.V.2	Nibaviridae	Ninavirus	Ninavirus	239	40889	PRJNA32810
01.SH1_10N.V.239	39			ninaduae			2
15.332.B._10N.239.312.A	15.332.B._10N.V.2	Nibaviridae	Ninavirus	Ninavirus	239	40889	PRJNA32810
01.SH1_10N.V.239	39			ninaduae			2
19.332.A._10N.239.312.A	19.332.A._10N.V.2	Nibaviridae	Ninavirus	Ninavirus	239	40889	PRJNA32810
01.SH1_10N.V.239	39			ninaduae			2
2.332.A._10N.239.312.A0	2.332.A._10N.V.23	Nibaviridae	Ninavirus	Ninavirus	237	40889	PRJNA32810
1.SH1_10N.V.237	7			ninaduae			2
2.332.B._10N.239.312.A0	2.332.B._10N.V.23	Nibaviridae	Ninavirus	Ninavirus	237	40889	PRJNA32810
1.SH1_10N.V.237	7			ninaduae			2
40.332.A._10N.239.312.A	40.332.A._10N.V.2	Nibaviridae	Ninavirus	Ninavirus	282	42318	PRJNA32810
01.SH1_10N.V.282	82			ninatria			2
40.332.B._10N.239.312.A	40.332.B._10N.V.2	Nibaviridae	Ninavirus	Ninavirus	282	42318	PRJNA32810
01.SH1_10N.V.282	82			ninatria			2

40.332.C._10N.239.312.A	40.332.C._10N.V.2	<i>Nibaviridae</i>	<i>Ninavirus</i>	<i>Ninavirus</i>	282	42318	PRJNA32810
01.SH1_10N.V.282	82			<i>ninatria</i>			2
40.332.D._10N.239.312.A	40.332.D._10N.V.2	<i>Nibaviridae</i>	<i>Ninavirus</i>	<i>Ninavirus</i>	282	42318	PRJNA32810
01.SH1_10N.V.282	82			<i>ninatria</i>			2
41.332.A._10N.239.312.A	41.332.A._10N.V.2	<i>Nibaviridae</i>	<i>Ninavirus</i>	<i>Ninavirus</i>	288	42316	PRJNA32810
01.SH1_10N.V.288	88			<i>ninatria</i>			2
41.332.B._10N.239.312.A	41.332.B._10N.V.2	<i>Nibaviridae</i>	<i>Ninavirus</i>	<i>Ninavirus</i>	288	42317	PRJNA32810
01.SH1_10N.V.288	88			<i>ninatria</i>			2
41.332.C._10N.239.312.A	41.332.C._10N.V.2	<i>Nibaviridae</i>	<i>Ninavirus</i>	<i>Ninavirus</i>	288	42318	PRJNA32810
01.SH1_10N.V.288	88			<i>ninatria</i>			2
41.332.D._10N.239.312.A	41.332.D._10N.V.2	<i>Nibaviridae</i>	<i>Ninavirus</i>	<i>Ninavirus</i>	288	42318	PRJNA32810
01.SH1_10N.V.288	88			<i>ninatria</i>			2
42.332.A._10N.239.312.A	42.332.A._10N.V.2	<i>Nibaviridae</i>	<i>Fabiennevirus</i>	<i>Fabiennevirus</i>	282	40897	PRJNA32810
01.SH1_10N.V.282	82			<i>fabienne-duae</i>			2
42.332.B._10N.239.312.A	42.332.B._10N.V.2	<i>Nibaviridae</i>	<i>Fabiennevirus</i>	<i>Fabiennevirus</i>	282	40897	PRJNA32810
01.SH1_10N.V.282	82			<i>fabienne-duae</i>			2
42.332.C._10N.239.312.A	42.332.C._10N.V.2	<i>Nibaviridae</i>	<i>Fabiennevirus</i>	<i>Fabiennevirus</i>	282	40897	PRJNA32810
01.SH1_10N.V.282	82			<i>fabienne-duae</i>			2
42.332.D._10N.239.312.A	42.332.D._10N.V.2	<i>Nibaviridae</i>	<i>Fabiennevirus</i>	<i>Fabiennevirus</i>	282	40897	PRJNA32810
01.SH1_10N.V.282	82			<i>fabienne-duae</i>			2
43.332.A._10N.239.312.A	43.332.A._10N.V.2	<i>Fatimavirid</i>	<i>Lisavirus</i>	<i>Lisavirus</i>	262	63173	PRJNA32810
01.SH1_10N.V.262	62	<i>ae</i>		<i>lisaduae</i>			2
43.332.B._10N.239.312.A	43.332.B._10N.V.2	<i>Fatimavirid</i>	<i>Lisavirus</i>	<i>Lisavirus</i>	262	63173	PRJNA32810
01.SH1_10N.V.262	62	<i>ae</i>		<i>lisaduae</i>			2
45.332.A._10N.239.312.A	45.332.A._10N.V.2	<i>Nibaviridae</i>	<i>Fabiennevirus</i>	<i>Fabiennevirus</i>	262	41452	PRJNA32810
01.SH1_10N.V.282	82			<i>fabiennetria</i>			2
45.332.B._10N.239.312.A	45.332.B._10N.V.2	<i>Nibaviridae</i>	<i>Fabiennevirus</i>	<i>Fabiennevirus</i>	282	41452	PRJNA32810
01.SH1_10N.V.282	82			<i>fabiennetria</i>			2
46.332.B._10N.239.312.A	46.332.B._10N.V.2	<i>Nibaviridae</i>	<i>Fabiennevirus</i>	<i>Fabiennevirus</i>	282	41452	PRJNA32810
01.SH1_10N.V.282	82			<i>fabiennetria</i>			2
47.332.A._10N.239.312.A	47.332.A._10N.V.2	<i>Nibaviridae</i>	<i>Fabiennevirus</i>	<i>Fabiennevirus</i>	282	41488	PRJNA32810
01.SH1_10N.V.282	82			<i>fabiennequattu</i>			2
				<i>or</i>			
48.332.A._10N.239.312.A	48.332.A._10N.V.2	<i>Nibaviridae</i>	<i>Fabiennevirus</i>	<i>Fabiennevirus</i>	282	41488	PRJNA32810
01.SH1_10N.V.282	82			<i>fabiennequattu</i>			2
				<i>or</i>			

48.332.B._10N.239.312.A	48.332.B._10N.V.2	Nibaviridae	Fabiennevirus	Fabiennevirus	282	41488	PRJNA32810
01.SH1_10N.V.282	82			fabiennequattu or			2
6.332.A._10N.239.312.A0	6.332.A._10N.V.23	Nibaviridae	Ninavirus	Ninavirus	237	40889	PRJNA32810
1.SH1_10N.V.237	7			ninaduae			2
7.332.B._10N.239.312.A0	7.332.B._10N.V.23	Nibaviridae	Ninavirus	Ninavirus	239	40889	PRJNA32810
1.SH1_10N.V.239	9			ninaduae			2
8.332.A._10N.239.312.A0	8.332.A._10N.V.23	Nibaviridae	Fabiennevirus	Fabiennevirus	282	41488	PRJNA32810
1.SH1_10N.V.282	8			fabiennequattu or			2
8.332.B._10N.239.312.A0	8.332.B._10N.V.23	Nibaviridae	Ninavirus	Ninavirus	238	40889	PRJNA32810
1.SH1_10N.V.238	8			ninaduae			2
8.332.C._10N.239.312.A0	8.332.C._10N.V.23	Nibaviridae	Ninavirus	Ninavirus	239	40889	PRJNA32810
1.SH1_10N.V.239	9			ninaduae			2
9.332.A._10N.239.312.A0	9.332.A._10N.V.23	Nibaviridae	Ninavirus	Ninavirus	238	40889	PRJNA32810
1.SH1_10N.V.238	8			ninaduae			2
9.332.B._10N.239.312.A0	9.332.B._10N.V.23	Nibaviridae	Ninavirus	Ninavirus	238	40889	PRJNA32810
1.SH1_10N.V.238	8			ninaduae			2
2.263.O_10N.286.54.F7_10N.255	2.263.O_10N.255	Fatimavirid ae	Sebastianoviru s	Sebastianoviru s sebastianoduo	255	59340	PRJNA32810 2
2.263.O_10N.286.54.F7_10N.262	2.263.O_10N.262	Fatimavirid ae	Sebastianoviru s	Sebastianoviru s sebastianounu s	262	59725	PRJNA32810 2
1.281.O_10N.286.54.F7	1.281.O	Fatimavirid ae	Sebastianoviru s	Sebastianoviru s sebastianounu s	286	59297	PRJNA32810 2
1.283.A_10N.286.55.A1	1.283.A	Fatimavirid ae	Sebastianoviru s	Sebastianoviru s sebastianotres	286	59530	PRJNA32810 2
1.269.O_10N.286.54.A6	1.269.O	Fatimavirid ae	Sebastianoviru s	Sebastianoviru s sebastianoduo	286	59738	PRJNA32810 2
1.267.O_10N.286.54.A1	1.267.O	Fatimavirid ae	Sebastianoviru s	Sebastianoviru s	286	59414	PRJNA32810 2

				<i>sebastianounu</i>			
				<i>s</i>			
1.270.A_10N.286.54.A8	1.270.A	<i>Fatimavirid</i>	<i>Sebastianoviru</i>	<i>Sebastianoviru</i>	286	59294	PRJNA32810
		<i>ae</i>	<i>s</i>	<i>s</i>			2
				<i>sebastianounu</i>			
				<i>s</i>			
1.143.O_10N.261.55.C8	1.143.O	<i>Nibaviridae</i>	<i>Jacobvirus</i>	<i>Jacobvirus</i>	261	44527	PRJNA32810
				<i>jacobduo</i>			2
1.127.O_10N.286.52.E12	1.127.O	<i>Nibaviridae</i>	<i>Jacobvirus</i>	<i>Jacobvirus</i>	286	44915	PRJNA32810
				<i>jacobunus</i>			2
4.233.O_10N.286.52.E12	4.233.O_10N.V.26	<i>Nibaviridae</i>	<i>Jacobvirus</i>	<i>Jacobvirus</i>	269	44468	PRJNA32810
_10N.V.269	9			<i>jacobduo</i>			2
7.233.O_10N.286.52.E12	7.233.O_10N.V.28	<i>Nibaviridae</i>	<i>Jacobvirus</i>	<i>Jacobvirus</i>	287	44915	PRJNA32810
_10N.V.287	7			<i>jacobunus</i>			2
4.233.O_10N.286.52.E12	4.233.O_10N.V.29	<i>Nibaviridae</i>	<i>Jacobvirus</i>	<i>Jacobvirus</i>	290	44916	PRJNA32810
_10N.V.290	0			<i>jacobunus</i>			2